Computer Simulation Studies of Water States in Perfluoro Polyether Reverse Micelles: Effects of Changing the Counterion†

Sanjib Senapati and Max L. Berkowitz*

Department of Chemistry, University of North Carolina at Chapel Hill, Chapel Hill, North Carolina 27599

Received: March 8, 2004; In Final Form: May 26, 2004

We performed molecular dynamics computer simulations to study the effect of counterions on the structural and dynamical properties of water pool enclosed by a reverse micelle containing ionic surfactants. Our simulations were performed on a system containing PFPE surfactants, water, and supercritical carbon dioxide. We chose NH_4^+, Na^+, and Ca^{++} to be the counterions. The results of the simulations showed that structural and dynamical properties of water in the pool created by the micellar system depend on the type of the counterion. We observed that the orientational dynamics of water inside the PFPE reverse micelles was slower as compared to the dynamics in bulk water or in an ionic aqueous solution irrespective of the type of the counterion present in the solution. The calculations showed that water dynamics got slower as we progressed from the NH_4^+ ion to the Na^+ ion and to the Ca^{++} ion. Finally, we observed the existence of water bridges connecting ions and charged headgroups in our simulations. These bridges contribute significantly into the slow orientational dynamics of water.

I. Introduction

Aqueous reverse micelles (RMs) contain nanometer-sized pools of water stabilized in a hydrophobic solvent by a surfactant coat. The structural and dynamical properties of water in these pools was intensely studied, partially due to their biological relevance.[1] A large body of experimental work using different techniques, such as flourescence probe measurements,[2,3] IR and Raman spectroscopy,[4,5] NMR,[6,7] electron spin resonance,[6] and differential scanning calorimetry measurements,[6,8] was performed to unravel the thermodynamic and structural properties of confined water. These experiments suggested that water in the pool can be mostly divided into two populations: bound water and free water. Fluorescence spectroscopy,[9−13] picosecond emission spectroscopy,[14] dielectric measurements,[15,16] femtosecond resolution,[17] and pulsed NMR studies[18] of the water pool confined in RMs and/or next to biomolecules have indicated the presence of dynamical modes in water that are much slower than the ones found in the bulk phase. Computer simulation methods have also been employed to explore the properties of the water pool in a RM. The first attempt to study a RM using molecular dynamics (MD) simulation was made by Brown and Clarke.[19] They observed that water molecules adopt a specific orientation and directly bond with the headgroup anions. Therefore, their study already gave an indication of the presence of bound water in reverse micellar aggregates. Linse[20] had carried out a molecular level simulation of an aqueous reverse micellar model system. The results showed that the structure of interfacial water was strongly perturbed and that the rate of rotational motion was significantly reduced. Tobias and Klein[21] have investigated the microscopic properties of a calcium carbonate/calcium sulfonate reverse micellar aggregate in nonpolar solvents. They concluded that the structure of the micelle is independent of the solvent and, on the average, water molecules are tightly bound to the surface of the micelle. This again was an indication of the presence of bound water in micellar aggregates. Faeder and Ladanyi[22] conducted a simulation study of the interior of model aqueous RMs. Their results suggested that the interfacial water is immobilized by a strong interaction with the ionic components at the interface. In a separate article,[23] they reported simulation results for the solvation dynamics of a diatomic solute in model RMs of varying sizes. In agreement with the experiment, they observed that the solvation response in RM becomes faster as the micellar size increases but that most of the effect occurs in the slower diffusive portion of the response. Salaniwal et al.[24] performed MD simulations of a dichain surfactant/water/carbon dioxide system and investigated various structural properties of the aggregates. They also followed the aggregation dynamics of the same ternary mixtures leading to a rapid and spontaneous self-assembly into aggregates that resemble RMs.[25] Their results revealed that water molecules in the interfacial region undergo a strong orientational motion in response to the presence of the electric field emanating from the ionic components, while water molecules near the center of the pool exhibit a hydrogen-bonded network similar to the one found in bulk water. Recently, we reported on the structure of a reverse micellar aggregate composed of a dichain phosphate fluorosurfactant in a water in CO_2 microemulsion. By combining data from the MD simulation and SANS (small angle neutron scattering) experiments, we have estimated the size and shape of the RM.[26] In a follow-up publication,[27] we, using MD simulations, examined the structure and dynamics of water in the various regions of the interior pool. We observed a dramatic slowing down of the rotational dynamics of interfacial water, although a bulk water domain was also found at the center of the aggregated core. We concluded that strong interactions of interfacial water molecules with the surfactant headgroups are mostly responsible for this slowing down, which is consistent with the findings related to the dynamics of water in other constraint environments.[9,14,27−29] While a large effort has been made to study the properties of water, few attempts have been made to study the effects of counterions on the water dynamics in a RM.[11,12,30,31] Levinger

† Part of the special issue "Tomas Baer Festschrift".

10.1021/jp048954p CCC: $27.50
Published on Web 07/27/2004

and co-workers[11,12] have investigated the change in water dynamics in AOT [Aerosol-OT, sodium bis(2-ethylhexyl) sulfosuccinate] RMs as a function of the type of the surfactant countercation, replacing Na^+ by K^+ and Ca^{++} and NH_4^+. From the solvation dynamics measurements data, Levinger and collaborators concluded that the Na^+ ion in AOT RMs is responsible for reducing a large fraction of the water motion in these environments. The counterion effect on the properties of water encased in ionic reverse micellar aggregates was also investigated by the ^1H NMR measurements.[30] This study showed that water proton spin−lattice relaxation rates increase on going from Na^+ to Ca^{++} and Mg^{++}, which means that the average correlation time of the encased water molecules increases with an increase in the polarization effects of the cations. Very recently, Faeder et al.[31] presented results from a MD simulation study of the effects of counterion type on the properties of the water pool in RMs. They found that several structural and dynamical properties of the water pool were strongly affected by the counterion. The changes resulted from the difference in the interactions between the counterion and the charged headgroups and/or the water solvent molecules. Efforts have also been made to elucidate the micellar structure and stability by varying the counterion type.[11,12,32−35] These studies (predominantly on AOT-based RM) revealed that various properties of a micelle depend strongly upon the identity of the counterion. For example, performing SANS experiments, Eastoe et al.[32] have shown that spherical AOT-based RMs transform to a cylindrical structure on substituting Na^+ countercation by transition metal divalent cations. RMs with alkali metal cations, on the other hand, remain spherical over the same range of water content.[32] SANS measurements of the ternary $Ca(AOT)_2/D_2O$/decane system by Capuzzi et al.[33] also revealed the formation of spherical water droplets similar in size to the one in NaAOT RMs. These results were supported by the data obtained from the dynamic light scattering experiments performed by Levinger and co-workers.[12] Levinger and co-workers[11] also showed that NH_4AOT- and NaAOT-based systems contain micelles of the same size and shape for the same w_0 value. A Fourier transform infrared study of the states of water in AOT-based RMs was carried out by Temsamani et al.,[34] and the whole sequence of alkali metal counterions was tested in their experiments. This investigation suggested that the amount of bound water in the headgroup region does not depend markedly on the counterion size. However, conductivity[35] and NMR self-diffusion measurements[35] showed that the microstructure of the ternary $Ca(AOT)_2$/water/*n*-decane system differs from the corresponding NaAOT system. In the present work, we examine the effect of the counterion identity on the structure and stability of a fluorosurfactant-based RM and on the structure and kinetics of the enclosed water pool. The micellar systems of interest in our work are composed of anionic perfluoropolyether carboxylate surfactant $CF_3-[O-CF_2-CF(CF_3)]_3-O-CF_2-COO^-$ (PFPECOO$^-$), water, and supercritical carbon dioxide. The different countercations used in the calculations are NH_4^+, Na^+, and Ca^{++}. A picture of the surfactant anion PFPECOO$^-$ is presented in Figure 1. We use MD simulation techniques to study micellar systems with a water to surfactant mole ratio (W_o) equal to 8.4. In a previous article[36] (paper 1), we presented the MD simulation results for the structural properties of the aqueous RM containing PFPECOO$^-NH_4^+$ surfactant in supercritical CO_2 with a W_o value of 8.4. Our simulation results showed an excellent agreement with experimental data and offered detailed information on the shape and structure of the system. Because we intended to perform a realistic simulation of a RM, we used a detailed molecular level description of all of the species. The results of paper 1 can be summarized as follows: the RM remained stable over the 5 ns time period of the simulation. The radius of the aqueous core obtained from the simulation was 19.2 ± 0.5 Å. The area per surfactant headgroup was calculated to be ≈70 Å^2. The calculated value of micelle eccentricity and visual inspection implied that the RM in our simulation was essentially spherical. Direct observation of the micellar shape fluctuations, the time evolution of the eccentricity, and the time evolution of the core radius indicated the stability of the micellar shape in the time scale of the simulation. The results also implied that about 89% of the ammonium counterions formed contact ion pairs with the headgroup atoms and that the interfacial water molecules penetrated the headgroup surface.

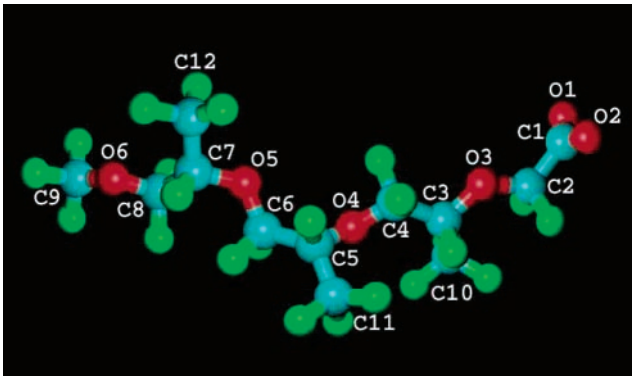

Figure 1. Balls and sticks representation of the surfactant anion PFPECOO$^-$ structure. The color scheme is as follows: red balls are for oxygens, cyan balls are for carbon atoms, and green balls are for fluorine atoms.

TABLE 1: LJ Parameters for the Counterions

atom type	σ_{ii} (Å)	ϵ_{ii} (kJ/mol)	atom type	σ_{ii} (Å)	ϵ_{ii} (kJ/mol)
N	3.250	0.71200	Na	3.328	0.01159
H	0.000	0.00000	Ca	3.052	1.92376

II. Model and Simulation Details

We performed three detailed MD simulations of aqueous RMs containing a polyether-based anionic fluorosurfactant in supercritical carbon dioxide. These three simulated systems differ by their countercation type. The countercations in our simulations are NH_4^+, Na^+, and Ca^{++}, respectively, for systems 1, 2, and 3. The OPLS set of intermolecular parameters[37] has been used to model NH_4^+ counterions. These parameters were shown to reproduce the experimental heat of solution and hydration numbers of ammonium ion in water. The five site model of the ammonium ion consists of one Lennard−Jones (LJ) site on the central N atom and five sites for point charges. The N−H distance is 1.01 Å, and the H−N−H angle is 109.47° with k_θ = 146.44 kJ/(mol rad^2). The site charges are −0.40 and 0.35, respectively, on N and H atoms. For Na^+ and Ca^{++} ions, we have used the potential parameters due to Aqvist.[38] These parameters reproduce the observed free energies of hydration and the ion−water radial distribution functions and have been included within standard Amber parameter files. The LJ parameters for the counterions are tabulated in Table 1. The SPC/E model[39] was chosen to describe the water molecules. The SPC/E model is a well-tested and widely used model for liquid water, which has been shown to give a good description of liquid water at both ambient and supercritical conditions. The rigid EPM2 model[40] proposed by Harris and Yung is used to describe CO_2. This model accurately reproduces the experi-

mental critical point and liquid−vapor coexistence curve and is being widely used. It is a three site model with each site represented by a LJ sphere with an embedded central point charge. We follow an all atom approach to model the anionic part $PFPECOO^-$ of the surfactant. The consistent valence force field[41−43] (CVFF) parameters were used to describe the intermolecular and intramolecular interactions involving the surfactant anions. The CVFF force field has been successfully applied to study the rheological behavior of confined branched and linear perfluropolyethers and hydrocarboxylic acids.[43] The same force field has also been used to model $PFPECOO^-$ anion at the water/CO_2 planar interface.[44] To calculate the values of the point charges, we used Accelrys' Material Studio software[42] with the CVFF force field. The detailed procedure used to build the RM can be found in paper 1. The three systems that we simulated contained 554 water molecules, 66 surfactant molecules, and 6359 CO_2 molecules placed in a cubic box at 25 °C and 200 bar pressure. The values for the temperature, pressure, and W_o are the same as the values present in the NMR experiment of the water/$PFPECOO^-NH_4^+$/CO_2 system by Nagashima et al.[45] We started our simulations from an aggregated configuration in which we distributed the surfactant molecules around the periphery of a sphere containing water molecules. The surfactants had their headgroups pointed inward and their tails solvated in CO_2 pointed outward. The countercations were randomly added inside the sphere of water. To enable volume variation, the simulations were performed in the NPT ensemble, using the Nose−Hoover thermostat and barostat.[46] Both the thermostat and barostat relaxation times were set to 0.5 ps. For each system, an equilibration simulation of 500 ps was performed before a production run of 5 ns. Periodic boundary conditions were employed in all directions. The calculation of the long-range Coulombic forces was performed using the smooth particle mesh Ewald (SPME) method.[47] The real space part of the Ewald sum and LJ interactions was cut off at 10 Å. We have also simulated a system containing pure bulk water at the same temperature and pressure as in simulations of micellar systems, so that the behavior of water in the confined system can be compared with that in the bulk phase. For bulk water, the simulation was carried out in a cubic box containing 216 particles. For the bulk system, periodic boundary conditions were applied in all three directions, the minimum image convention was used for the short-range interactions, and the SPME method was employed for the long-range interactions. The bulk water system was equilibrated for 200 ps, and then, the production run was continued for 1 ns. In addition, we simulated three other systems each composed of one cation and 216 water molecules also at 25 °C and 200 bar pressure. The cations in the respective system were NH_4^+, Na^+, and Ca^{++}. These systems were simulated to examine the effect of cations on water dynamics in the bulk phase and to compare the results with water dynamics in a micellar environment. Each system was equilibrated for 500 ps followed by a 2 ns production run. All of the simulations in this work were carried out using the DLPOLY[48] MD simulation package.

III. Results and Discussion

A. Micellar Size and Shape. The geometry of a RM can be characterized by the size and the shape of its aqueous core. A useful statistical measure of the size of a micellar core is its radius of gyration, R_g. We calculated R_g for the aqueous core of all three micellar systems by using the following formula

$$R_g^2 = \sum_i m_i(r_i - r_o)^2 / \sum_i m_i \qquad (1)$$

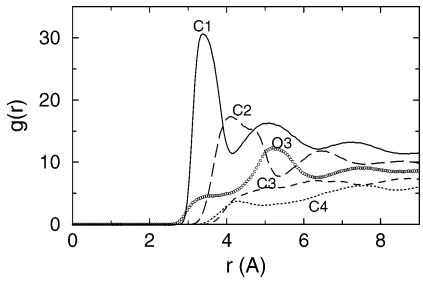

Figure 2. Radial distribution functions between water oxygen and various atoms along the $PFPECOO^-NH_4^+$ surfactant backbone. Atom notations are the same as in Figure 1.

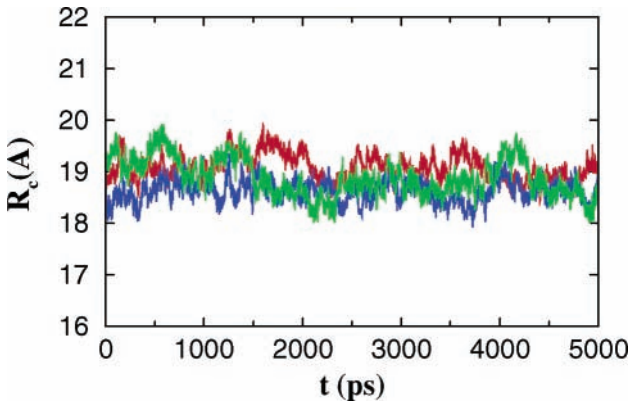

Figure 3. Time evolution of the core radii of RMs with NH_4^+ (red line), Na^+ (blue line), and Ca^{++} (green line) counterions during the 5 ns of the production run.

where *i* includes the water molecules in the core, the counterions, the carboxylate group, the adjacent CF_2 group (C2), and the first ether oxygen (O3) in each of the surfactant tails. Here, m_i is the mass and r_i is the distance of atom *i* from the center of mass r_o of the aggregated core. The reason for including the first CF_2 group and the first ether oxygen in the calculation is that they are found to be well-solvated in water. This can be seen from the pair radial distribution functions (rdf) of water oxygen (O_w) with the central atom of various groups present in the surfactant tails. In Figure 2, we have plotted the rdfs for the pairs of O_w−C1, O_w−C2, O_w−O3, O_w−C3, and O_w−C4 in system 1 (for the atom notation, see Figure 1). The trend is very similar for systems 2 and 3; therefore, the data for these systems are not included in the figure. The figure clearly shows that water penetrates the headgroup surface and solvates the carboxylate group, the first CF_2 group, and the first ether oxygen group of the surfactant tail. Water density then gradually diminishes, and any group beyond O3 does not contribute much to the calculation of R_g. The radius of gyration of a spherical aggregate with uniform mass distributions is related to its radius R_c by a simple relation: $R_g^2 = 3/5R_c^2$. Although the uniform mass assumption does not hold in our case, this relationship, which is also used by the experimentalists, can provide us with an estimate of the core radii of the RMs. The time histories of the core radii of the RMs during the entire 5 ns of the production run for the three systems are presented in Figure 3. We observe that the cores are stable, since the figure indicates that the values of R_c are stable in time. The average values of R_c that we obtained from the simulations are 19.2 ± 0.5, 18.6 ± 0.7, and 18.9 ± 0.9 Å, respectively, for systems 1, 2, and 3. The value of R_c = 19.2 Å is in good agreement with the experimental value of 20 Å obtained for the aqueous droplet in the $PFPECOO^-NH_4^+$/water/carbon dioxide system.[45] The stability of the aggregates can be further tested by examining the time

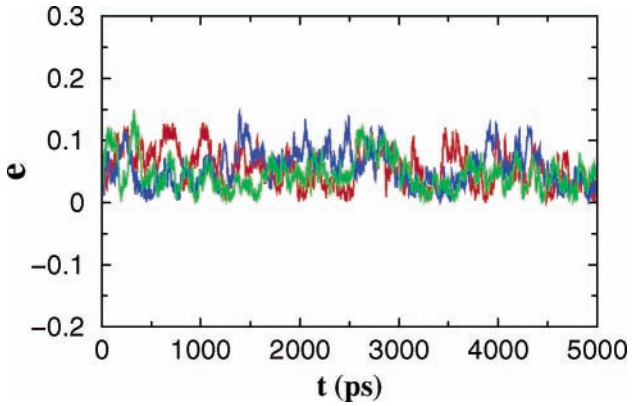

Figure 4. Time evolution of the eccentricities of RMs with NH_4^+ (red line), Na^+ (blue line), and Ca^{++} (green line) counterions during the 5 ns of the production run.

evolution of their eccentricity, *e*. Eccentricity can also provide us with a quantitative measure of the aggregate shape. We define the micelle eccentricity as:[24]

$$e = 1 - \frac{I_{\min}}{I_{\text{avg}}} \tag{2}$$

where $I_{\min}$ is the moment of inertia of the micelle along the *x*-, *y*-, or *z*-axis with the smallest magnitude and I_{avg} is the average of all three moments of inertia. The time evolution of the eccentricities during the final 5 ns for all three systems is plotted in Figure 4. The eccentricities for systems 1, 2, and 3 are found to fluctuate around the average values of 0.05, 0.06, and 0.05, respectively. For a perfect sphere, the eccentricity should be zero. The values of *e* in our systems indicate that the aggregates are essentially spherical. We also confirm our previous observation that micelles are stable in time, since the values of the eccentricity are quite stable. The issue of a shape of a RM containing different counterions deserves some special consideration. For example, while a group of authors[32,12] reported that $Ca(AOT)_2$-based RM forms spherical aggregates, another group[35] found it to be a nonspherical aggregate maker. For micelles, general considerations show that ions with large hydration radii display a smaller degree of counterion binding, therefore producing lower screening of the electrostatic repulsions between the headgroups. This results in a decreased tendency to undergo a sphere-to-rod micellar shape transition.[49] What is the situation with Ca^{++} ions in our simulations? As we move to the next subsection, we will see that Ca^{++} ions reside close to the headgroup surface. In general, it is important to realize that a strong competition exists between counterion−water and counterion−headgroups coulomb interactions. Carboxylate headgroups of our surfactants with two negatively charged oxygens interact more effectively with Ca^{++} than a water oxygen does. This brings Ca^{++} ions in close proximity to the headgroups and, therefore, effectively reduces the charge density at the surface. Nevertheless, micelles with Ca^{++} counterions retain their spherical shape in our simulations.

B. Water Structure. Exploring properties of water in a confined environment is an important field of current research. In this study, we have investigated the influence of counterions on the structure and dynamics of water confined inside the RM. To compare the properties of water that is in the vicinity of the headgroup surface with the properties of water at the center of the aqueous core, we have divided the water region in each micellar system into two primary subregions. The first subregion contains bound or interfacial water molecules (these interact directly with the ionic components of the surfactants); the second subregion contains more mobile water molecules (these are further away from the interface). The boundary of the two subregions was selected by looking at the position of the first solvation shell observed in the rdf between the carboxylate headgroup carbon and the water oxygen. Figure 5 shows the rdfs for all three micellar systems. Thus, bound water molecules in systems with NH_4^+, Na^+, and Ca^{++} counterions are those that lie within 4.1, 4.8, and 4.9 Å in C1−O_w rdf (the distances at first minima). In their turn, free water molecules were divided into three subcategories: free I molecules, which lie between the first and the second minima in the respective rdfs; free II water molecules situated between the second minimum and 9.5 Å; and free III water molecules that are located beyond 9.5 Å. The idea of subdividing the free water molecules is to find the region where the water behavior matches the bulk. The choice of 9.5 Å for the beginning of region III was determined by calculating the hydrogen bond distribution in this region. It was found that this distribution for water beyond 9.5 Å matches the one in bulk water. The structure of water in different regions of the pool inside the RM depends on the composition in these regions. Therefore, we calculated the local densities of counterions as a function of distance from the effective surface formed by the carboxylate carbon atoms (the algorithm used to obtain these profiles was recently described by our group elsewhere[52]). The profiles are shown in Figure 6. This figure clearly shows that all three types of cations have a tendency to form contact ion pairs and that calcium ions stay closest to the headgroup surface, followed by sodium and ammonium ions. The sharp and narrow peak observed for Ca^{++} counterions also indicates that in this case almost all of the ions remain ion paired with the headgroups. In the cases of NH_4^+ and Na^+ ions, we observe that quite a few ions dissociate from the surface and dissolve in the interior of the water pool. The location of the ions and water molecules in the water pool of the micelle is

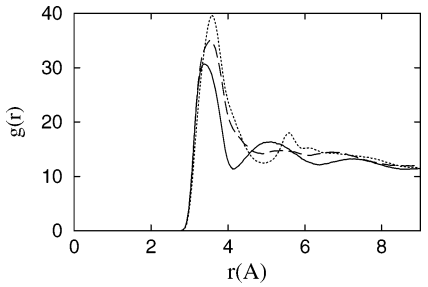

Figure 5. Radial distribution functions for a carboxylate carbon−water oxygen pair for RMs with NH_4^+ (solid line), Na^+ (dashed line), and Ca^{++} (dotted line) counterions.

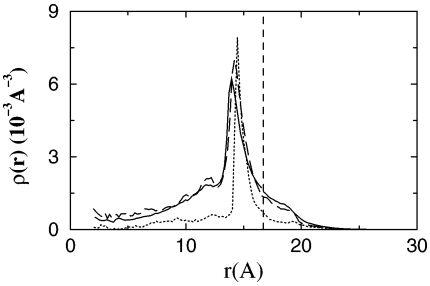

Figure 6. Number density profiles for the NH_4^+ (solid line), Na^+ (dashed line), and Ca^{++} (dotted line) ions in the corresponding RMs with respect to the effective surface at 16.7 Å (shown by a dashed vertical line). The effective surface is formed by the carboxylate carbon atoms.

TABLE 2: Number of Hydrogen Bonds Per Water Molecule in Various Regions[a]

cation type	bound	free I	free II	free III
NH_4^+	1.723 ± 0.014	2.758 ± 0.032	3.441 ± 0.019	3.523 ± 0.035
Na^+	1.869 ± 0.021	3.075 ± 0.042	3.409 ± 0.084	3.529 ± 0.010
Ca^{++}	1.946 ± 0.042	3.249 ± 0.019	3.531 ± 0.016	3.577 ± 0.010

[a] Error ranges are determined by calculating hydrogen bond distributions for 10 separate 100 ps segments.

determined by a competition between the ion-charged headgroup interaction, the ion−water interaction, and the charged headgroup−water interaction. Ions with a high charge density like Ca^{++} ions (charge density order: $Ca^{++} > Na^+ > NH_4^+$) can strongly interact with the carboxylate headgroups, and this may bring them closest to the headgroups. We now return to the study of water properties in various regions of the water pool. To investigate the water hydrogen bond distribution, we adopted a geometric definition of hydrogen bonding.[50,51] According to this definition, a pair of water molecules is hydrogen bonded if the oxygen−oxygen distance is less than 3.5 Å and simultaneously the oxygen−oxygen−hydrogen angle is less than 30°. Table 2 shows the distribution of an average number of hydrogen bonds (H-bonds) per water molecule at various locations. The results show that the counterions modify the water−water H-bond environment significantly. A similar conclusion was drawn by Chandra[51] in a study of the effects of ion atmosphere on the H-bond structure and dynamics in aqueous electrolyte solutions. It is also seen from Table 2 that the average number of water−water H-bonds is always larger for the RM with Ca^{++} counterions as compared to micelles with NH_4^+ or Na^+ counterions. This is somewhat surprising, since the ions having the highest charge densities are expected to be the most disruptive of the water−water hydrogen-bonding pattern. However, the difference nearly disappears for the free III water molecules that are located far away from the interface. The average number of hydrogen bonds for water in this region matches very well the value of 3.60 determined for bulk water at the specified temperature and pressure, particularly in the case of the RM with a Ca^{++} counterion. To explain this observation about the water−water hydrogen-bonding pattern, we observe that in the RM with calcium counterions there is only half a number of counterions as compared to the other two systems. This explains why in the interfacial region the average number of water−water hydrogen bonds is larger in the case of micelles with Ca^{++} counterions (see Table 2). The water molecules in the bound region of micelles with calcium are present in a larger amount and therefore can be somewhat better hydrogen bonded to each other. The observed higher number of H-bonds for free I and free II water molecules is due to the fact that almost all Ca^{++} ions reside in the bound water region and therefore are less effective in disrupting the water−water hydrogen-bonding network in free water regions. We have also seen (Table 2) that the value for the average number of H-bonds for the free III water region in micelles with ammonium and sodium counterions is slightly smaller than the bulk value of 3.60. This is due to the fact that a small percentage of ammonium and sodium ions dissociates from the interface and dissolves in the interior (see Figure 6). Our analysis of hydrogen-bonding pattern in different regions shows that the connection between the number of hydrogen bonds and the density of counterions is to some extent trivial; the presence of a larger number of counterions produces a smaller number of hydrogen bonds. To find the intrinsic probability of forming hydrogen bonds, we calculated the ratio of the number of hydrogen bonds to the number of nearest water neighbors. As we can see from the values of this ratio, which are presented in Table 3, the intrinsic probability is nearly independent of the number and nature of counterions. The carboxylate headgroups of the surfactant molecules contain oxygen atoms that are capable of forming hydrogen bonds with the first shell water hydrogens. We have studied this capability by computing the water to headgroup hydrogen bonds. To describe a water to headgroup hydrogen bond, we have used the same geometric definition of hydrogen bonds as for the water−water case; that is, a water and a headgroup are hydrogen bonded if a headgroup oxygen−water oxygen distance is not greater than 3.5 Å and simultaneously the headgroup oxygen−water hydrogen angle is not greater than 30°. The average number of water to headgroup hydrogen bonds for RM with NH_4^+, Na^+, and Ca^{++} ions was computed to be 1.01, 0.66, and 0.50, respectively. This result is in accordance with the fact that Ca^{++} ions approach closely to the interface (Figure 6) and destabilize the water to headgroup hydrogen bonds. Also, because of its high charge density, Ca^{++} ions cause strong electrostatic ordering of nearby water, thus breaking the headgroup−water hydrogen bonds. The bulkiest and low charge denisty NH_4^+ ions, on the other hand, remain further away from the interface and allow water to be hydrogen bonded to the headgroups. Figure 7 shows the number density profiles of water in the three micellar systems as a function of the distance from the headgroup surface. Again, the numbers in this figure were obtained by calculating the local densities of water as a function of the distance from the effective surface formed by the carboxylate carbon atoms. The density profiles from this figure show a layered structure of water, which is consistent with the previous studies on liquid structure at liquid/liquid interfaces.[22,27,53,54] Figure 7 indicates that a significant amount of water penetrates the hydrophobic region and hydrates this region to some extent. There are a few other distinct features in this figure, which are to be noted. Thus, we notice that the first peak observed in the system with the Na^+ counterion is shifted to the left with respect to the first peak observed for systems with the NH_4^+ or Ca^{++} counterions and that the first peak height has the largest value for the system with the Na^+ ion. We also observe that in the case of the Ca^{++}

TABLE 3: Ratio of the Number of Hydrogen Bonds and the Number of Nearest Water Neighbors in Various Regions[a]

cation type	bound	free I	free II	free III
NH_4^+	0.415 ± 0.003	0.519 ± 0.003	0.565 ± 0.004	0.580 ± 0.007
Na^+	0.387 ± 0.005	0.508 ± 0.010	0.546 ± 0.017	0.575 ± 0.005
Ca^{++}	0.379 ± 0.006	0.527 ± 0.007	0.566 ± 0.006	0.577 ± 0.005

[a] Error ranges are determined by calculating hydrogen bond distributions for 10 separate 100 ps segments.

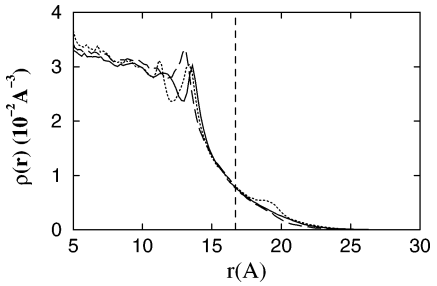

Figure 7. Number density profiles for water in RMs with the NH_4^+ (solid line), Na^+ (dashed line), and Ca^{++} (dotted line) counterions with respect to the effective surface formed by the carboxylate carbon atoms. The effective surface located at 16.7 Å is shown by a dashed vertical line.

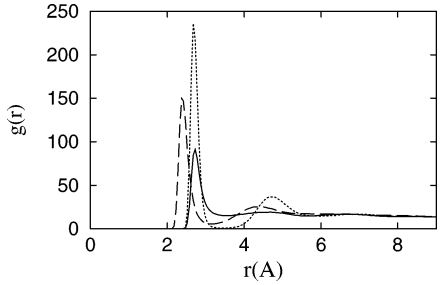

Figure 8. Radial distribution functions for counterion−water oxygen pairs in respective RMs. The solid, dashed, and dotted lines are for the NH_4^+, Na^+, and Ca^{++} counterions.

counterion there is a distinct peak in the water density distribution for water that is located in the interior of the hydrophobic region. To explain these observations, we return to Figure 6. According to this figure, sodium ions are located closer to the headgroups surface than ammonium ions. Therefore, sodium ions remove the water molecules from the interface more effectively than ammonium ions. This is why we observe a shift in the first peak of the water density distribution in the RM with sodium ions. However, such a shift is not observed in the water density distribution for the RM with calcium ions, although calcium ions are the closest to the surface. In this case, the distribution shows the presence of a distinct peak located inside the hydrophobic region. Because calcium ions strongly bind to the micellar surface, they disturb the surface more significantly. As a result, water molecules can penetrate into the hydrophobic region, instead of moving away from the surface. To see how ions disturb the surrounding water molecules, we present in Figure 8 the counterion−water pair distribution functions for all three systems. This figure clearly implies that the charge densities of ions govern their interactions with water. Calcium ions with the highest charge density bound more water molecules than sodium or ammonium ions. The calculated hydration numbers for NH_4^+, Na^+, and Ca^{++} ions are 3.7, 3.7, and 5.1, respectively. These are smaller than the hydration numbers of 5.7, 5.8, and 8.8 waters obtained from the separate simulations of one counterion in 216 water molecules at 25 °C and 200 bar pressure. A large reduction in the coordination number confirms the presence of contact ion pairs between the carboxylate headgroups and the counterions in our systems. A similar observation was also reported in the previous studies.[24,26] Thus, as we can see, the network of the bound water molecules is strongly influenced by the presence of surfactant headgroups and counterions. This influence is not that prominent for the free water molecules, but in certain cases, the free water molecules behave quite differently from the bulk water. Next, we will consider how the structural changes influence the change in the water dynamics.

C. Water Dynamics. A variety of experimental studies[9−14] have indicated that water dynamics in a reverse micellar aggregate contains slow modes that relax on the 100−1000 ps time scale. This dynamic is remarkably slower than the subpicosecond relaxation dynamics observed in the ordinary bulk water. Recent computer simulation studies[27,29,55] also demonstrated that water dynamics in the micellar interfacial region slows down several hundred to thousand times as compared to the dynamics in bulk water. As the recent research showed, the presence of slow motion in the water pool of a RM is mainly due to the water−headgroup interactions at the interface.[9,14,27−29] A handful of attempts has also been made to examine the effects of counterions on the water dynamics in a RM.[11,12,31] To study the effect of counterions on the water

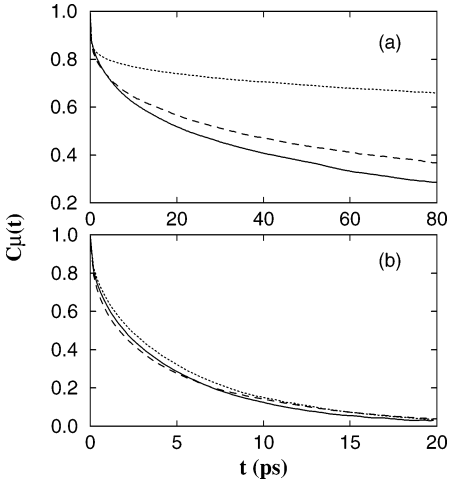

Figure 9. Single dipole autocorrelation functions for water molecules in RMs with NH_4^+ (solid line), Na^+ (dashed line), and Ca^{++} (dotted line) counterions: (a) for bound water and (b) for free III water. The curves for bound water are cut at 80 ps to show clearly the differences between the three systems.

dynamics, we calculated the water dipole autocorrelation function, $C_\mu(t)$ in our three micellar systems. The results of these calculations are presented in Figure 9. Figure 9a displays the data for bound water molecules, and Figure 9b displays the data for free III water molecules. The single water dipole autocorrelation function, which is a characteristic measure of the reorientational motion of a fluid, can be defined as

$$C_\mu(t) = \langle \mu_i(t) \cdot \mu_i(0) \rangle / \langle \mu_i(0) \cdot \mu_i(0) \rangle \qquad (3)$$

where $\mu_i(t)$ is the dipole vector of i-th molecule at time t. The plots in Figure 9 are obtained by averaging over the water molecules that have large residence times in their respective shells. In other words, to calculate $C_\mu(t)$, we pay attention only to those water molecules that remain in their respective shells continuously for a long enough time. In this, we follow a prescription originally proposed by Bagchi and collaborators.[29] As one would expect, this restricts our choice, since fewer water molecules will qualify for our consideration. Note that we also want to pick up a fair number of molecules in every shell to get a good averaging statistic. Thus, we choose 20 water molecules that stay in the interfacial region of micelles with NH_4^+, Na^+, and Ca^{++} ions continuously for a time period of 100, 200, and 1000 ps, respectively. The larger residence time of water in the first shell of Ca^{++} or Na^+ ion-based RM itself implies an influence of ionic headgroups on water dynamics. The average number of water molecules considered for plotting Figure 9b is 15, and they are found to be in the free III region continuously for 20 ps in each case. The relaxation time of the free III water molecules is similar in all of the systems because of a weak influence of the interface on the water molecules in this region. The data on the time correlation functions (tcf) indicate that the reorientational motion of water molecules in bound and free regions and in all three micellar systems is highly nonexponential and involves a slowly decaying tail. Therefore, we fitted the correlation functions to a multiexponential function of the following form

$$C_\mu(t) = \sum_{i=1} c_i \exp(-t/\tau_i) \qquad (4)$$

where $\sum_{i=1}$, $c_i = 1$, and τ_i is the time constant for the decay of the i-th component. We observed that one needs to use at least

TABLE 4: Fit Parameters of the Time Correlation Functions, $C_\mu(t)$, for Water in Various Environments

(a) Bound Water

system	cation type	c_1	τ_1 (ps)	c_2	τ_2 (ps)	c_3	τ_3 (ps)
RM	NH_4^+	0.14	0.28	0.26	8.62	0.60	105.37
RM	Na^+	0.19	0.43	0.22	12.34	0.59	170.65
RM	Ca^{++}	0.18	0.44	0.11	27.78	0.71	1000.07

(b) Free III Water

system	cation type	c_1	τ_1 (ps)	c_2	τ_2 (ps)
RM	NH_4^+	0.31	0.49	0.69	5.98
RM	Na^+	0.44	0.84	0.56	7.10
RM	Ca^{++}	0.30	0.60	0.70	6.45

three exponents to fit the behavior of the autocorrelation function for bound water. The fitting parameters are tabulated in Table 4a. The behavior of the autocorrelation function of free III water can be described by just two exponents, and the parameters for these are given in Table 4b. The decay of the bulk water shows the expected behavior—after a transient period, the decay is exponential with a time constant close to 5 ps. The calculated time constant is somewhat larger than the time constant previously reported for bulk water,[56] probably due to different state conditions (25 °C and 200 bar pressure) and a higher density of water in our system. The data in Table 4 indicate that the relaxation of the interfacial water is significantly slower than that of bulk water. The relaxation of free III water is similar to the bulk water. The relaxation of free I and free II water falls into the intermediate range. We also observe that the diffusive components of bound water molecules relax extremely slow and that the relaxation time for the slowest mode is 2−3 orders of magnitude larger as compared to the relaxation time in bulk water. A similar slowing down in water dynamics was observed by Levinger and collaborators[10−12] in their solvation dynamics measurements performed on AOT-based RMs. The relaxation time constant of the slowest mode in bound water increases from 105 to 170 ps and to 1000 ps when we move from micelles with NH_4^+ ions to micelles with Na^+ and to Ca^{++} counterions. The change in the values of the time constants implies that counterions are responsible for reducing a significant fraction of the water motion in a reverse micellar environment. A similar conclusion was drawn by Riter et al.[11] based on their solvation dynamics measurements performed on counterion-exchanged AOT-based RMs. In a study of the effects of ion atmosphere on hydrogen bond dynamics in aqueous electrolyte solutions, Chandra[51] also found that the orientational relaxation of water varies with the ion type. To understand how the presence of micellar environment influences the dynamics of water next to the ion, we compared the micellar system results with the results obtained from the simulations of isolated NH_4^+, Na^+, and Ca^{++} ions in bulk water. We observed that the decay of $C_\mu(t)$ for water molecules next to an isolated cation is always faster than the decay in a micellar environment. This implies that although counterion−water interactions play a significant role in the slowing down of water dynamics, in a micellar environment, other factors also affect the dynamics of water. Indeed, recent results reported by us[27,55] and other groups[9,14,22,28,29] indicated that interactions of water with the headgroups and the geometrical confinement of water are among the factors responsible for the slow dynamics of water. In search of a reason for a substantial change in the relaxation time of bound water molecules as a function of counterion type, we consider here a new factor, namely, the presence of water bridges in a micellar environment, which may contribute significantly to the slow dynamics of water. Therefore, we checked the possibility of

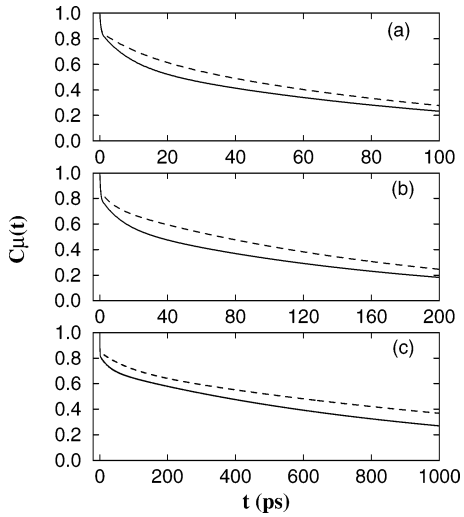

Figure 10. Relaxation of dipolar correlation functions for water molecules in RMs with (a) NH_4^+, (b) Na^+, and (c) Ca^{++} counterions. The solid lines represent the relaxation of bound water molecules, and dashed lines represent the relaxation of bridged water molecules. All lines are fits to the data via eq 4.

water forming a bridge between the counterions and the ionic headgroups. In such a bridge, the water oxygen points toward a positively charged counterion and water hydrogen forms a H-bond with an electronegative headgroup atom. In determining the bridged water molecules in our systems, we consider only those water molecules that reside in the first shell of a counterion, and from these water molecules, we then choose only those that form at least one H-bond with the carboxylate (headgroup) oxygen atoms. We compute $C_\mu(t)$ for these bridged water molecules and also perform the corresponding multiexponential fit to the computed data. The results of the fits are shown in Figure 10. (Instead of computed values, we plot the corresponding fits, since the computed values for bridged water molecules were somewhat noisy due to a small number of molecules over which the averaging was done.) The solid lines in Figure 10 represent the relaxation of bound water molecules, and the dashed lines represent the relaxation of bridged water molecules. Figure 10a−c displays the decay of tcf for water molecules in micelles with NH_4^+, Na^+, and Ca^{++} counterions. We found that out of 20 bound water molecules that we considered in Figure 9, at least seven of them form bridges. The dynamics of these bridged water molecules is extremely slow; therefore, they contribute significantly to the overall slow dynamics of water in the interfacial region. To get a quantitative estimate of the relaxation of bridged water molecules, we calculated the average orientational correlation time, τ_{avg}, defined as

$$\tau_{avg} = \int_0^\infty dt\, C_\mu(t) \tag{5}$$

Because our correlation function was calculated only up to a finite time, to estimate the behavior of this function at longer times, we again fitted the dipolar autocorrelation function to a multiexponential function as given by eq 4. From eq 5 and using eq 4 for the extrapolation of the long-time tail region, we obtained the following estimates for the values of average orientational correlation times: 78, 134, and 1086 ps for bridged water molecules and 65, 103, and 713 ps for bound water molecules in micelles with NH_4^+, Na^+, and Ca^{++} ions, respectively. This means that the relaxation of bridged molecules is 20−45% slower than bound water molecules (remember that

bridged water molecules constitute a subgroup of bound molecules). Notice that the relaxation times for water molecules around Ca^{++} ions and water molecules that participate in bridges in RMs with Ca^{++} counterions are the longest. It is, however, worth emphasizing that the relaxation times and their averages given above are just estimates that depend on the quality of fitting, extrapolation, and statistics. (We observed small quantitative changes in the average orientational correlation time when we fitted the orientational correlation functions to the sum of four exponentials. Qualitative results remained the same. Therefore, both previous and present simulations clearly show that water next to hydrophilic surfaces and/or next to charged ions is substantially slowed.)

IV. Summary and Conclusions

In this paper, we report on a computational study of the effect of counterions on the structural and dynamical properties of a water pool enclosed by a RM containing PFPE surfactants. Three different systems were studied, which differed by the type of counterions that were chosen. We chose NH_4^+, Na^+, and Ca^{++} to be the counterions. We observed that structural and dynamical properties of water in the pool created by the micellar system depend on the type of the counterion. Subtle differences in the hydrogen-bonding pattern were noticed when we changed the nature of the counterion. We observed that the orientational dynamics of water inside the PFPE RMs was slower as compared to the dynamics in bulk water or in an ionic aqueous solution irrespective of the type of the counterion present in the solution. We also observed that the dynamics got slower as we progressed from the NH_4^+ ion to the Na^+ ion and finally to the Ca^{++} ion. These observations are consistent with the conclusions reached by Levinger and collaborators in their experimental work performed on the AOT RMs. In their interpretation of the vibrational spectroscopy measurements, Moran et al.[57] proposed that water bridges connecting ions and charged headgroups exist in AOT-based micelles. We directly observed the existence of such water bridges in our simulations. These bridges display long orientational relaxation times and contribute significantly into the slow orientational dynamics of water. Although it may be harder to perform experimental studies on reverse PFPE micelles in water/carbon dioxide systems, as compared to the study of AOT RMs in water/oil systems, we believe that properties of water pool inside the micelle are rather universal. Our belief is supported by an agreement between the data directly obtained from our simulations and the conclusions inferred from the experimental measurements.

Acknowledgment. This work was supported by the Kenan Center for the Utilization of Carbon Dioxide in Manufacturing and the STC Program of the National Science Foundation under Agreement CHE-9876674. The simulations were performed on an IBM SP machine at the North Carolina Supercomputing Center. This work is dedicated to Tomas Baer, with congratulations.

References and Notes

(1) *Reverse Micelles: Biological and Technological Relevance of Amphiphilic Structures in Apolar Media*; Luisi, P. L., Straub, B. E., Eds.; Plenum: New York, 1984.

(2) Belletete, M.; Lachapelle, M.; Durocher, G. *J. Phys. Chem.* **1990**, *94*, 5337.

(3) De, T. K.; Maitra, A. *Adv. Colloid Interface Sci.* **1995**, *59*, 95.

(4) D'Aprano, A.; Lizzio, A.; Turco Liveri, V.; Aliotta, F.; Vasi, C.; Migliardo, P. *J. Phys. Chem.* **1988**, *92*, 4436.

(5) Jain, T. K.; Varshney, M.; Maitra, A. *J. Phys. Chem.* **1989**, *93*, 7409.

(6) Hauser, H.; Haering, G.; Pande, A.; Luisi, P. L. *J. Phys. Chem.* **1989**, *93*, 7869.

(7) Heatley, F. *J. Chem. Soc., Faraday Trans. 1* **1989**, *85*, 917.

(8) Boned, C.; Peyrelasse, J.; Moha-Ouchanne, M. *J. Phys. Chem.* **1986**, *90*, 634.

(9) Levinger, N. E. *Curr. Opin. Colloid Interface Sci.* **2000**, *5*, 118.

(10) iter, R. E.; Willard, D. M.; Levinger, N. E. *J. Phys. Chem. B* **1998**, *102*, 2705.

(11) Riter, R. E.; Undiks, E. P.; Levinger, N. E. *J. Am. Chem. Soc.* **1998**, *120*, 6062.

(12) Pant, D.; Riter, R. E.; Levinger, N. E. *J. Chem. Phys.* **1998**, *109*, 9995.

(13) Zhang, J.; Bright, F. V. *J. Phys. Chem.* **1991**, *95*, 7900.

(14) (a) Sarkar, N.; Datta, A.; Das, S.; Bhattacharyya, K. *J. Phys. Chem.* **1996**, *100*, 15483. (b) Sarkar, N.; Das, K.; Datta, A.; Das, S.; Bhattacharyya, K. *J. Phys. Chem.* **1996**, *100*, 10523. (c) Das, S.; Datta, A.; Bhattacharyya, K. *J. Phys. Chem. A* **1997**, *101*, 3299. (d) Datta, A.; Mandal, D.; Pal, S. K.; Bhattacharyya, K. *J. Phys. Chem. B* **1997**, *101*, 10221.

(15) Grant, E. H.; McClean, V. E. R.; Nightingale, N. R. V.; Sheppard, R. J.; Chapman, M. J. *Bioelectromagnetics* **1986**, *7*, 151.

(16) Fukuzaki, M.; Miura, N.; Sinyashiki, N.; Kunita, D.; Shiyoya, S.; Haida, M.; Mashimo, S. *J. Phys. Chem.* **1995**, *99*, 431.

(17) Pal, S. K.; Peon, J.; Zewail, A. H. *Proc. Natl. Acad. Sci. U.S.A.* **2002**, *99*, 1763.

(18) (a) Urry, D. W.; Peng, S.; Xu, J.; McPherson, D. T. *J. Am. Chem. Soc.* **1997**, *119*, 1161. (b) Bolton, P. S. *J. Phys. Chem.* **1995**, *99*, 17061.

(19) Brown, D.; Clarke, J. H. R. *J. Phys. Chem.* **1988**, *92*, 2881.

(20) Linse, P. *J. Chem. Phys.* **1989**, *90*, 4992.

(21) Tobias, D. J.; Klein, M. L. *J. Phys. Chem.* **1996**, *100*, 6637.

(22) Faeder, J.; Ladanyi, B. M. *J. Phys. Chem. B* **2000**, *104*, 1033.

(23) Faeder, J.; Ladanyi, B. M. *J. Phys. Chem. B* **2001**, *105*, 11148.

(24) (a) Salaniwal, S.; Cui, S. T.; Cochran, H. D.; Cummings, P. T. *Langmuir* **2001**, *17*, 1773. (b) Salaniwal, S.; Cui, S. T.; Cochran, H. D.; Cummings, P. T. *Ind. Eng. Chem. Res.* **2000**, *39*, 4543.

(25) (a) Salaniwal, S.; Cui, S. T.; Cochran, H. D.; Cummings, P. T. *Langmuir* **2001**, *17*, 1784. (b) Salaniwal, S.; Cui, S. T.; Cochran, H. D.; Cummings, P. T. *Langmuir* **1999**, *15*, 5188.

(26) Senapati, S.; Keiper, J. S.; DeSimone, J. M.; Wignall, G. D.; Melnichenko, Y. B.; Frielinghaus, H.; Berkowitz, M. L. *Langmuir* **2002**, *18*, 7371.

(27) Senapati, S.; Berkowitz, M. L. *J. Chem. Phys.* **2003**, *118*, 1937.

(28) Senapati, S.; Chandra, A. *J. Chem. Phys.* **1999**, *111*, 1223.

(29) (a) Balasubramanian, S.; Bagchi, B. *J. Phys. Chem. B* **2002**, *106*, 3668. (b) Balasubramanian, S.; Pal, S.; Bagchi, B. *Curr. Sci.* **2002**, *82*, 845. (c) Pal, S.; Balasubramanian, S.; Bagchi, B. *J. Chem. Phys.* **2002**, *117*, 2852.

(30) Zhu, X. X.; Bardez, E.; Dallery, L.; Larrey, H.; Valeur, B. *New J. Chem.* **1992**, *16*, 973.

(31) Faeder, J.; Albert, M. V.; Ladanyi, B. M. *Langmuir* **2003**, *19*, 2514.

(32) Eastoe, J.; Towey, T. F.; Robinson, B. H.; Williams, J.; Heenan, R. K. *J. Phys. Chem.* **1993**, *97*, 1459.

(33) Capuzzi, G.; Pini, F.; Gambi, C. M. C.; Monduzzi, M.; Baglioni, P. *Langmuir* **1997**, *13*, 6927.

(34) Temsamani, M. B.; Maeck, M.; Hassani, I. E.; Hurwitz, H. D. *J. Phys. Chem. B* **1998**, *102*, 3335.

(35) Caboi, F.; Capuzzi, G.; Baglioni, P.; Monduzzi, M. *J. Phys. Chem. B* **1997**, *101*, 10205.

(36) Senapati, S.; Berkowitz, M. L. *J. Phys. Chem. B* **2003**, *107*, 12906.

(37) Jorgensen, W. L.; Gao, J. *J. Phys. Chem.* **1986**, *90*, 2174.

(38) Aqvist, J. *J. Phys. Chem.* **1990**, *94*, 8021.

(39) Berendsen, H. J. C.; Grigera, J. R.; Straatsma, T. P. *J. Phys. Chem.* **1987**, *91*, 6269.

(40) Harris, J.; Yung, K. H. *J. Phys. Chem.* **1995**, *99*, 12021.

(41) Dauber-Osguthorpe, P.; Roberts, V. A.; Osguthorpe, J.; Wolff, D. J.; Genest, M.; Hagler, A. T. *Proteins: Struct. Funct. Genet.* **1988**, *4*, 31.

(42) *Discover User Guide Part I*; Biosym Technologies: CA, 1993.

(43) (a) Koike, A. *J. Phys. Chem. B* **1999**, *103*, 4578. (b) Koike, A.; Yoneya, M. *J. Chem. Phys.* **1996**, *105*, 6060.

(44) da Rocha, S. R. P.; Johnston, K. P.; Rossky, P. J. *J. Phys. Chem. B* **2002**, *106*, 3250.

(45) Nagashima, K.; Lee, C. T.; Xu, B.; Johnston, K. P.; DeSimone, J. M.; Johnson, C. S. *J. Phys. Chem. B* **2003**, *107*, 1962.

(46) (a) Nose, S. *J. Chem. Phys.* **1984**, *81*, 511. (b) Hoover, W. G. *Phys. Rev. A* **1985**, *31*, 1695.

(47) Essmann, U.; Perera, L.; Berkowitz, M. L.; Darden, T.; Lee, H.; Pedersen, L. G. *J. Chem. Phys.* **1995**, *103*, 8577.

(48) Smith, W.; Forester, T. R. *DLPOLY*, 2.12 version; CCLRC; Daresbury Laboratory: 1999.

(49) Srinivasan, V.; Blankschtein, D. *Langmuir* **2003**, *19*, 9946.

(50) (a) Luzar, A.; Chandler, D. *Phys. Rev. Lett.* **1996**, *76*, 928. (b) Luzar, A.; Chandler, D. *Nature (London)* **1996**, *379*, 53.
(51) Chandra, A. *Phys. Rev. Lett.* **2000**, *85*, 768.
(52) Pandit, S. A.; Bostick, D.; Berkowitz, M. L. *J. Chem. Phys.* **2003**, *119*, 2199.
(53) Fernandes, P. A.; Cordeiro, M. N. D. S.; Gomes, J. A. N. F. *J. Phys. Chem. B* **1999**, *103*, 8930.
(54) da Rocha, S. R. P.; Johnston, K. P.; Westacott, R. E.; Rossky, P. J. *J. Phys. Chem. B* **2001**, *105*, 12092.
(55) Bruce, C. D.; Senapati, S.; Berkowitz, M. L.; Perera, L.; Forbes, M. D. E. *J. Phys. Chem. B* **2002**, *106*, 10902.
(56) Chandra, A.; Ichiye, T. *J. Chem. Phys.* **1999**, *111*, 2701.
(57) Moran, P. D.; Bowmaker, G. A.; Cooney, R. P. *Langmuir* **1995**, *11*, 738.